Available online at www.sciencedirect.com
ScienceDirect
New Astronomy Reviews 50 (2006) 960–968
New Astronomy Reviews
www.elsevier.com/locate/newastrev

APEX-SZ first light and instrument status

M. Dobbs [g], N.W. Halverson [d,*], P.A.R. Ade [c], K. Basu [f], A. Beelen [a], F. Bertoldi [a,f], C. Cohalan [g], H.M. Cho [b], R. Güsten [f], W.L. Holzapfel [b], Z. Kermish [b], R. Kneissl [b], A. Kovács [f], E. Kreysa [f], T.M. Lanting [b], A.T. Lee [b,e], M. Lueker [b], J. Mehl [b], K.M. Menten [f], D. Muders [f], M. Nord [a,f], T. Plagge [b], P.L. Richards [b], P. Schilke [f], D. Schwan [b], H. Spieler [e], A. Weiss [f], M. White [b]

[a] *Argelander Institute for Astronomy, University of Bonn, Bonn, Germany*
[b] *University of California, Berkeley, CA, United States*
[c] *Cardiff University, Wales, UK*
[d] *University of Colorado, Boulder, CO, United States*
[e] *Lawrence Berkeley National Laboratory, Berkeley, CA, United States*
[f] *Max Planck Institute for Radio Astronomy, Bonn, Germany*
[g] *McGill University, Montréal, Canada*

Abstract

The APEX-SZ instrument is designed for the discovery and study of galaxy clusters at mm-wavelengths using the Sunyaev Zel'dovich effect. The receiver consists of 320 superconducting transition edge sensor (TES) bolometers cooled to 250 mK with the combination of a three stage He sorption fridge and mechanical pulse tube cooler. The detectors are instrumented with a frequency domain multiplexing readout system. The receiver is mounted on the 12 m APEX telescope located at 5100 m on the Atacama plateau in Chile. For the first light engineering deployment of December 2005, the receiver was configured with a 55 element wedge of the bolometers and operating in the 150 GHz atmospheric window. During the engineering run we achieved significant milestones in our instrumentation development efforts, including celestial observations with a monolithically fabricated TES bolometer array cooled with a mechanical cooler and successful implementation of a SQUID-based MHz AC-biased readout. These technology demonstrations point the way toward future large TES bolometer array instruments. Here we describe the results of this deployment and future plans for the APEX-SZ instrument.

PACS: 98.80.Es; 95.85.Bh; 98.65.Cw

Keywords: Cosmology; Observations; Galaxies; Clusters

Contents

* Corresponding author.
E-mail address: Nils.Halverson@Colorado.edu (N.W. Halverson).

1387-6473/$ - see front matter © 2006 Elsevier B.V. All rights reserved.
doi:10.1016/j.newar.2006.09.029

1. Introduction

The APEX-SZ galaxy cluster survey instrument is a 320 element transition edge sensor (TES) bolometer array receiver designed to conduct a large mass-limited survey of galaxy clusters using the Sunyaev-Zel'dovich (SZ) effect. The instrument was deployed for an engineering run and saw first light in December 2005 on the 12 m Atacama Pathfinder EXperiment (APEX) telescope. The APEX telescope was commissioned in September 2005 at its site in the Chilean Atacama desert; see Güsten et al. (2006a); Güsten et al. (2006b) for detailed descriptions of the APEX project. The APEX-SZ survey instrument is scheduled for its first science observing run in Fall 2006.

The Sunyaev-Zel'dovich effect (Sunyaev and Zeldovich, 1970) is a distortion of cosmic microwave background (CMB) photons as they pass through clusters of galaxies. The surface brightness of this effect is largely independent of redshift, allowing detection of galaxy clusters with mm-wavelength detectors at all redshifts at which clusters are present. APEX-SZ is a powerful new SZ survey instrument, with a mapping speed significantly faster than the present generation of SZ experiments. With APEX-SZ, we will survey 100–200 square degrees to an rms of 10 μK per arcminute pixel. We expect to discover and catalog thousands of previously unknown galaxy clusters in a mass-limited survey. This will enable us to study the evolution of structure formation in the universe and constrain cosmological parameters, such as the matter density and the dark energy equation of state, that are associated with structure formation.

A description of the instrument, including the receiver, telescope, Chajnantor site, optics, detectors, and readout is given in Section 2, the instrument configuration for the first engineering run is given in Section 3, first light instrument characterization, including instrument noise characterization and optical beam parameters, are described in Section 4, we discuss the current status and plans in Section 5, and conclude in Section 6.

2. The APEX-SZ instrument

The APEX-SZ instrument is an imaging array receiver incorporating monolithically fabricated transition-edge sensor (TES) bolometers. The initial configuration of band-defining filters is tuned to an observation frequency of 150 GHz (2 mm wavelength), with possible future observations at 90 and/or 220 GHz. The bolometer array consists of six triangular wedges, each containing 55 spiderweb absorber-coupled Al/Ti bilayer TES bolometers (Lee et al., 2003). A total of 320 detectors will be instrumented in the survey configuration. The detectors are cooled by the combination of a He pulse tube cooler and a three-stage He sorption refrigerator to a temperature of 250 mK. They are AC biased and read out by SQUID-based electronics with shunt-feedback (Spieler, 2002) for low impedance and increased dynamic range. The system is being upgraded to an 8-channel frequency-domain multiplexed (fMUX) readout for the upcoming Fall 2006 science run. The instrument is mounted in the Cassegrain receiver cabin of the APEX telescope. Reimaging optics in the Cassegrain cabin allow the APEX-SZ focal plane to instantaneously image a 22′ field of view (FOV) with 60″ FWHM beams. The receiver as installed in the APEX telescope is shown in Fig. 1.

2.1. Telescope and Chajnantor site

The Atacama Pathfinder EXperiment (APEX) telescope (Güsten et al., 2006; Güsten et al., 2006) is a 12-m diameter submillimeter telescope designed for observations up to 1.2 THz (250 μm). The telescope, is located near Cerro Chajnantor at an elevation of 5100 m, on the Atacama plateau adjacent to the Atacama Large Millimeter Array (ALMA) site in northern Chile. Designed and built by Vertex RSI, the APEX telescope is a prototype ALMA antenna, with the addition of two Nasmyth cabins, and is intended for single-dish observations with a complement of both heterodyne and bolometer array receivers. The primary mirror panel alignment has been measured with holography and aligned to an rms surface accuracy of 17–18 μm. The superb optical quality, along with arcsecond pointing accuracy and secondary mirror supports designed to minimize stray light scattering, make the telescope very well suited to a mm-wavelength SZ survey instrument.

The Chajnantor site has been well characterized as part of the ALMA site testing program, and has been found to have both low levels of precipitable water vapor and very good atmospheric stability (Radford and Holdaway, 1998; Lay and Halverson, 2000), both necessary for

Fig. 1. The APEX-SZ receiver installed in the APEX Cassegrain cabin in December 2005.

mm-wave low-contrast observations of the CMB and SZ effect on arcminute angular scales. The site has been successfully used for mm- and cm-wavelength CMB experiments (TOCO (Miller et al., 2002)), CBI (Padin et al., 2002). It is the chosen site for the Atacama Cosmology Telescope (ACT) (Kosowsky, 2003) and the CMB polarization experiments POLARBeaR and Q/U Imaging Experiment (QUIET). Excellent site conditions exist for most of the year. However, the "Bolivian winter," a weather pattern which transports moisture westward from the Bolivian Andes resulting in increased precipitable water vapor (PWV) levels and frequent precipitation, prevails from late December through March. This period is not ideal for a mm-wave SZ observations but proved useful for our engineering run and instrument characterization.

2.2. Optics

The design features of the APEX-SZ reimaging optics include a flat, telecentric *f*/2.3 focal plane, diffraction limited performance over a 22′ FOV, a cold (4 K) Lyot stop to limit spillover on the primary, and a cryostat angle of 30–45° from the telescope optical axis. This angle allows the use of a mechanical pulse-tube cooler, which must be kept within 30° of vertical during observations.

As shown in Fig. 2, the APEX-SZ focal plane is coupled to the sky via conical feedhorns and two 4 K high-density polyethylene (HDPE) lenses located inside the cryostat, plus three ambient temperature aluminum mirrors. This achieves a diffraction limited 22′ FOV. The $1.4f\lambda$ spaced feedhorns are arranged in a hex close-pack focal plane configuration. The first element of the APEX-SZ reflective reimaging optics design is a 1440 mm diameter off-axis paraboloid on the cabin floor 1970 mm below the Cassegrain focus. This is followed by a 620 mm folding flat

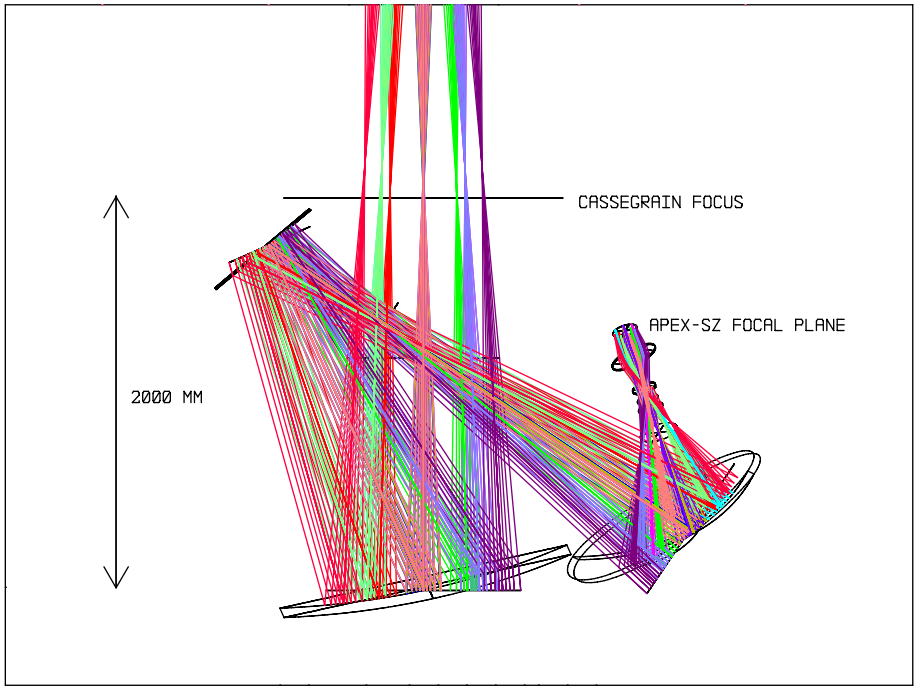

Fig. 2. The APEX-SZ reimaging optics layout. The Cassegrain focus, at top, is reimaged via a 1440 mm diameter paraboloid, 620 mm folding flat, and 980 mm × 1160 mm ellipsoid to an intermediate focus outside the receiver window, and a cold 4 K Lyot stop located inside the cryostat window. Two cold 4 K HDPE lenses collimate and re-image the light onto a *f*/1.4 telecentric focal plane.

and a 980 mm × 1160 mm ellipsoidal mirror near the reimaged focus that creates an image of the primary 800 mm from the mirror. This aperture image is used as a 4 K Lyot stop inside the receiver cryostat. Two HDPE lenses between the Lyot stop and focal plane create a flat, telecentric focal plane at *f*/1.4. All mirrors and lenses are conics, with no extra aspheric terms. The FOV is limited to $<22'$ by the 750 mm hole in the primary. The *72* mm Lyot stop diameter truncates the beam at ~0.8 of the primary diameter. This small-diameter Lyot stop allows the use of existing capacitive mesh filters for IR blocking. The 150 mm diameter cryostat vacuum window employs a two-inch thickness of Zotefoam which has negligible absorption at millimeter wavelengths.

2.3. Detectors

The entire APEX-SZ detector focal plane is fabricated in six triangular monolithic sections of 55 bolometers. Each element (Fig. 3) has a transition-edge sensor placed at the center of a 4 mm gold spiderweb absorber. This configuration gives an optical time constant of roughly 6–8 ms. The TES is a thin bilayer of aluminum and titanium, with film thicknesses tuned to give 470 mK superconducting transition temperature and size chosen to give 1.2 Ω normal resistance. The TES is physically coupled to a large, 3 μm thick ring of gold, which adds heat capacity to the bolometer slowing its electrical time constant for consistency with the optical response time. The average thermal conductance of the bolometers is set by a gold finger to be $\bar{G} \simeq 250\ \mathrm{pW/K}$.

2.4. Readout

The science deployment of APEX-SZ will use a frequency-domain multiplexer which requires only a single superconducting quantum interference device (SQUID) to read out a module of eight bolometers (Spieler, 2002; Lanting et al., 2004). All of the system elements were tested in the engineering run (see Section 3), allowing the full multiplexer to be deployed for the science observations. This considerably reduces the readout system cost and cold-component complexity.

A schematic diagram, Fig. 4, shows the basic components of the readout system. The bolometers are sinusoidally

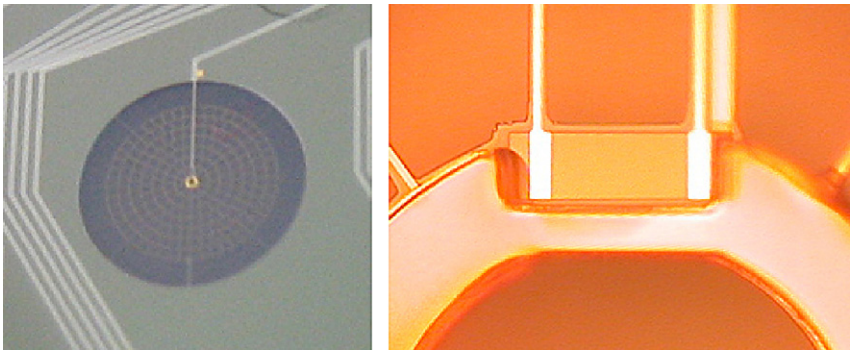

Fig. 3. Photograph (left) of one spiderweb bolometer on the 55 element APEX-SZ wedge. The transition edge sensor is at the center of the spiderweb and shown in the close-up photograph (right) with the circular gold ring visible in the bottom half of the photo.

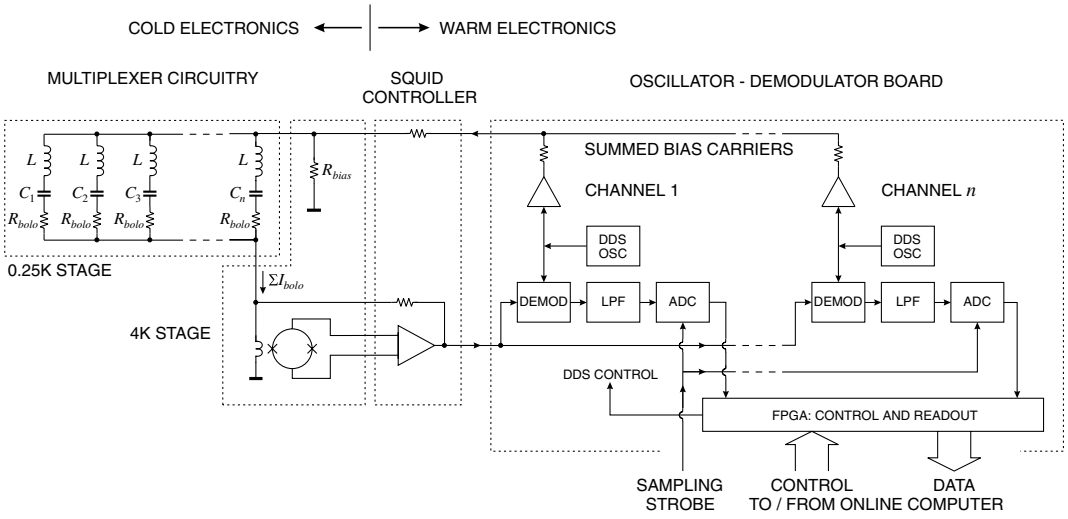

Fig. 4. The APEX-SZ readout system is shown in the science deployment frequency-domain multiplexer configuration. For the engineering run, all the elements of the readout system were in place, but the channels were not joined together in multiplexer mode (i.e., multiple bolometer channels are not joined together with the dashed lines in the diagram).

voltage biased at frequencies ranging from 300 kHz to 800 kHz. The biases are provided by a set of direct digital synthesizers with 12-bit amplitude accuracy and each bolometer in a readout module is biased at a different frequency. The TES is electrically biased in its superconducting transition. Negative electro-thermal feedback (Irwin, 1995) maintains a stable TES operating resistance and increases its linearity. The sky signal changes the bolometer resistance and amplitude modulates the current through the bolometer such that the signal from each bolometer is transferred to sidebands adjacent to its bias frequency. Thus, the signals from different bolometers within a module are uniquely positioned in frequency, so they can be summed and connected through a single wire to the input coil of a 100-element series array SQUID manufactured by NIST (Huber et al., 2001).

Each bolometer is part of a series-resonant LC circuit which is tuned to the appropriate bias frequency. This allows the bias frequencies for all bolometers in a module to be applied through a single wire, as the tuned circuit selects the appropriate frequency for each bolometer. Only two wires are needed to connect the bolometers of a readout module on the 0.25 K stage to the ~4 K stage on which the SQUIDs are mounted. The comb of amplitude modulated carriers at the SQUID output is transmitted to a bank of demodulators that mix the signals back down to base-band. The signals are then filtered and digitized, and all outputs in the array are sampled synchronously. More information about the readout system can be found in Ruhl et al. (2004).

3. Engineering deployment configuration

In December 2005 APEX-SZ was deployed to the APEX telescope site near Cerro Chajnantor. Three days of instrument characterization were possible before the telescope was shut down for Christmas and generator maintenance. In January 2006 an additional two weeks was allocated for instrument characterization, ending January 30. Storms throughout January reduced time available for useful sky-observations. While the Bolivian winter is not the ideal time for astronomical observations, it is sufficient for instrument characterization including measurements of beams with bright point sources, scan-synchronous spurious signals, detector noise properties, atmospheric fluctuations, and a general proof-of-concept for the instrument.

3.1. Instrument configuration for engineering deployment

For the engineering deployment, a staged version of the APEX-SZ receiver was installed. The configuration was chosen so that all the major systems of the receiver could be tested while still allowing for modifications of the detectors and other systems before the science deployment. A photograph of the receiver installed in its engineering configuration is shown in Fig. 1.

One of the six bolometer wedges, consisting of 55 TES bolometers, was installed and operating. All of the features of the frequency-domain multiplexed configuration shown in Fig. 4 were in-place for the engineering configuration, with the exception that the bolometer channels were not joined together above and below the inductor–capacitor-bolometer legs of the circuit (corresponding to the long dashed lines on the left in the figure). In this configuration, the series inductor and capacitor, which together resonate at the bias frequency, effectively tune out the inductance of the wires connecting the bolometer. The configuration is a step towards the fully multiplexed system, as the components we find most challenging (AC-bias, low noise mixing, cold high-Q notch filter) are all in place.

Of the 55 pixel channels, several were disconnected between the SQUID and TES to allow measurements of readout system stability and noise. Three additional channels suffered wiring faults, rendering them inoperative. This left 48 functioning pixels, of which ~43 were tuned, biased, and operating properly for a typical observation, including two "dark channels" with feedhorns covered.

The engineering run utilized the full APEX-SZ optics chain, providing single-color observations at 150 GHz. The receiver cabin mirrors were adjusted by micrometer during the cryogenic cool down period. The instrument saw first light December 23, 2005. The offsets for individual bolometer pixels were determined using raster scans of Mars, which appeared as a point source with an antenna temperature of ~5 K. With the offsets known, the optical system was focused by adjusting the position of the secondary mirror.

4. First light instrument characterization

4.1. Noise characterization

The characterization of end-to-end receiver noise was an important goal for this engineering run. This characterization allows for the validation of the detector and readout system, vibration environment during telescope motion, and RF shielding.

The expected noise contributions for one representative channel are shown in Table 1 and a measured noise spectrum is shown in Fig. 5. These data were recorded with

Table 1
The noise expectation for channel 'e7:rb7' with the closed receiver window providing a warm load

Noise source	Equation	NEP contribution aW/$\sqrt{\text{Hz}}$
Warm readout electronics	$3.3\text{pA}/\sqrt{\text{Hz}} \cdot V_{\text{bias}}$	10.
SQUID	$2.5\text{pA}/\sqrt{\text{Hz}} \cdot V_{\text{bias}}$	8.
Bolometer Johnson noise	$\sqrt{4\,k_{\text{B}} T_{\text{bolo}} P_{\text{elec}}}$	16.
Bolometer thermal phonon noise	$\sqrt{4\,k_{\text{B}} T_{\text{bolo}}^2 G_{\text{T}}}$	61.
Photon shot noise	$\sqrt{2\,h\nu P_{\text{incident}}}$	87.
Photon correlation noise	$\sqrt{\gamma \frac{P_{\text{incident}}^2}{\Delta\nu}}$	139.

Here k_{B} is the Boltzmann constant, h is Planck's constant, $\nu = 150$ GHz is the band center, $\Delta\nu = 23$ GHz is the bandwidth, $V_{\text{bias}} = 3\mu V_{\text{RMS}}$ and the other parameters are described in the text. G^{T} is the thermal conductance at the bolometer temperature, about 300 pW/K.

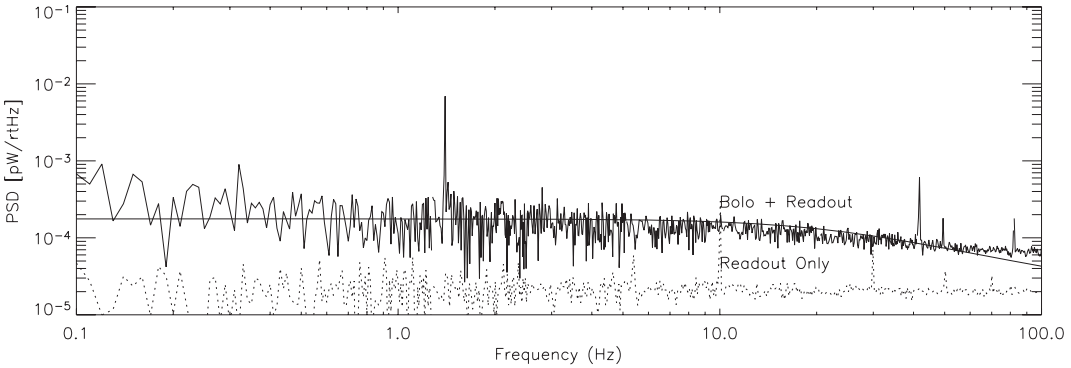

Fig. 5. Measured noise spectrum (solid line) for bolometer channel 'e7:rb7'. These data were recorded with the receiver window closed and the telescope slewing, so as to reproduce the vibration environment expected during science observations while excluding atmospheric fluctuations. The smooth curve is the theoretical expectation and the dashed line is the measured noise spectrum from a readout channel with no bolometer attached.

the receiver window closed and the telescope slewing, so as to reproduce the vibration environment while excluding atmospheric fluctuations. The total loading is calculated to be 48 pW, with $P_{\mathrm{elec}} = 10$ pW coming from electrical bias power and $P_{\mathrm{incident}} = 38$ pW coming from the hot warm load of the closed receiver window. The noise includes broadband white contributions from Johnson noise in the readout electronics, SQUID, and bolometer. These components are attenuated at high frequency by a 400 Hz anti-aliasing filter preceding the analog-to-digital converter in the readout chain. These white noise sources do not modulate the carrier and appear uncorrelated between the two sidebands of the carrier. The total white Johnson noise contribution is 20 $\mathrm{aW}/\sqrt{\mathrm{Hz}}$. Within the optical bandwidth of the bolometer, thermal phonon noise, photon shot noise, and photon correlation noise all modulate the bolometer resistance and dominate the noise spectra. To calculate the photon correlation noise we have arbitrarily assumed a correlation factor $\gamma = 0.3$. Refer to Lamarre (1986), Marcus Runyan et al. (2003) for more detailed discussions of photon correlations.

The noise expectation is superimposed on the noise spectrum measurement shown in Fig. 5. For these data the only processing is a 3rd order polynomial subtraction which removes the largest components of an overall temperature drift. The spectrum is in good agreement with expectation, considering the uncertainties in the parameters. The slight over-estimation of the noise may indicate the overall loading is slightly lower than assumed. A spike is visible at 1.4 Hz, corresponding to the pumping frequency of the pulse-tube cooler. This source is correlated across all channels and is easily removed. The noise spectrum for the SQUID readout system alone is obtained from a channel with no bolometer attached and also shown in Fig. 5.

Low frequency $1/f$ noise is visible below 1 Hz in this spectrum and attributed primarily to temperature drifts. This signal is largely correlated across the array and can be mitigated by subtracting a common mode signal. The sinusoidal voltage bias for the bolometers exhibits a low-frequency sideband that may contribute to $1/f$ noise, but its knee is considerably lower in frequency.

The APEX telescope is shared by several receivers and the assortment of electronic equipment can present a challenging RF-environment. During sky-observations in December and January occasional (few per minute) spikes and step functions were visible in the APEX-SZ pixel timestreams. These 'glitches' were correlated across the array and most frequent when the receiver window was open to the sky. RF-interference is suspected and steps are being taken to improve the RF-shielding between the optics chamber and detector/SQUID regions of the cryostat for the next deployment. The glitches can be flagged and removed from the timestreams.

4.2. Optical performance

During the engineering run, we characterized the optical performance of the instrument, including beam shapes, optical efficiency, optical loading, crosstalk, and the presence of atmospheric fluctuations in the data. Beam shapes, focus adjustments, and array pointing offsets were determined by raster scans of Mars, Jupiter, and Saturn. Optical loading was determined by analyses of skydip data, and observations of known loads, including Eccosorb disks and planets. Optical efficiencies across the array were estimated from comparison of known planet fluxes to calibrated optical power presented at the detectors. Finally, although weather conditions during the Bolivian winter observations were not optimal, we were able to preliminarily characterize atmospheric fluctuation power in the data, and start to develop tools for mitigating its effects.

At the best focus position, the array mean beamwidth was 59″, with a range of 48–75″, after deconvolution with the 35″ planet disk diameter, see left panel of Fig. 6. These measurements compare favorably with the 58″ mean and 51–70″ range predicted by ZEMAX physics optics propagation for a perfectly aligned optical system. Measured beamwidth variations are due to fitting uncertainties in the coarsely spaced raster pattern data and variations in optical aberrations across the wide FOV.

We created a combined beam map of Jupiter by co-adding beam maps of individual bolometers with appropriate

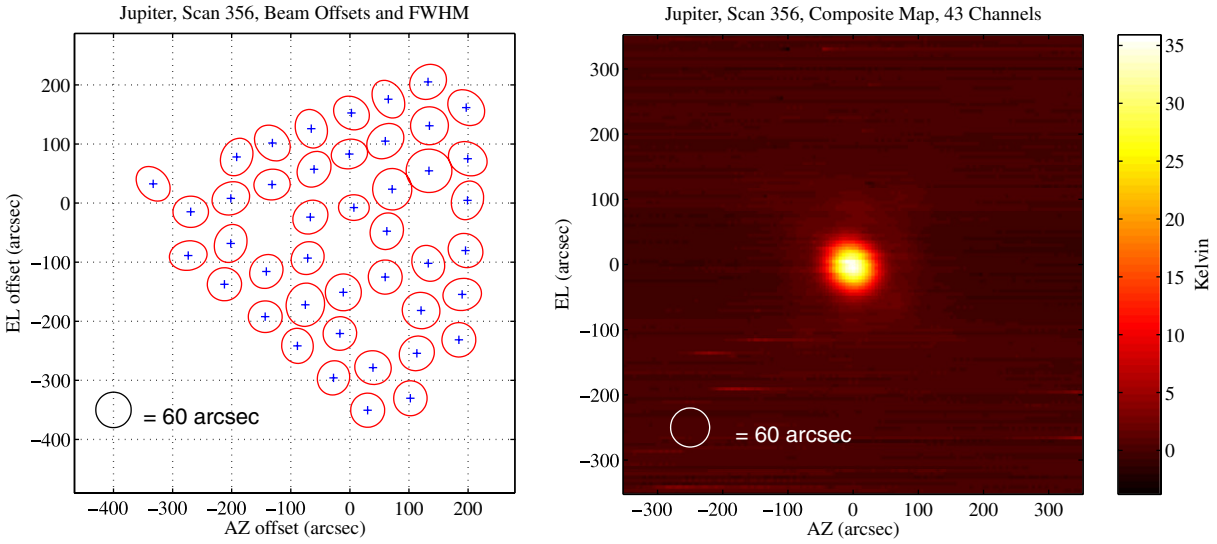

Fig. 6. (Left panel) Beam offsets and best fit FWHM ellipses determined from a raster observation of Jupiter at the secondary mirror best focus position. At this focus position, the mean beamwidth is 59″, with a range of 48–75″, after deconvolution with the 35″ planet disk diameter. Measured beamwidth variations are due to fitting uncertainties in the coarsely spaced raster pattern data and variations in optical aberrations across the wide FOV. (Right Panel) A composite beam map of Jupiter using 43 bolometer channels. Channel maps are combined with an angular offset determined from individual beam maps, and after calibration with the known brightness temperature of Jupiter convolved with the individual measured beam parameters. The composite beam map has a FWHM of ~60″ as expected, with reasonably well behaved sidelobes, although there is evidence of optical crosstalk (see text).

angular offsets and calibrations. The composite map (right panel of Fig. 6) has a resolution of ~60″, close to that expected. The sidelobes are reasonably well behaved, although there is evidence of optical crosstalk, discussed below. Laboratory measurements of the beam just outside the cryostat window also yielded beam patterns consistent with those predicted by ZEMAX.

Optical efficiency and loading were calculated from observations of known loads. Measurements prior to deployment, using a cold (77 K) neutral density filter in front of the dewar window, and a small 300 K Eccosorb disk yielded optical efficiency measurements of $\eta_{\rm opt} \sim 30\%$. However, measurements in the field based on unresolved planet observations yielded efficiencies $\eta_{\rm opt} \sim 10$–17%. During skydip measurements we also discovered significant crosstalk between light (sky viewing) pixels and dark pixels, with a ratio of 20% in dark-to-light pixel response. We hypothesize that ~0.6 of the power incident on a given bolometer cavity was radiated to and absorbed by other detectors on the wedge, thus accounting for the reduced measured optical efficiency from calculations based on point-like loads (planets) versus the lab measurements where the test load was resolved, and seen by adjacent pixels. Optical efficiency measurements using the Moon on dark detectors, and subsequent finite-element electromagnetic simulations were consistent with this. The simulations indicate the bolometer wedge's poor optical performance is due to low spiderweb sheet resistance of only 25 Ω/sq and a mistuned backshort distance of roughly 525 μm in silicon. We are altering the wedge and cavity geometry to reduce crosstalk and improve optical efficiency; see Section 5.

Optical loading measurements from skydip data yielded airmass brightness temperatures of 7, 15, and 30 K for pixels near the center of the array for three different nights, corresponding to atmospheric opacities of $\tau = 0.03$, 0.06, and 0.12, respectively. While reliable data from the telescope PWV monitor were not available, the derived opacities were consistent with observed weather conditions during the run. Observations were stopped frequently due to water precipitating on the primary. Extrapolating to a zero airmass loading we found loading on the order of 10 K due to the warm optics (primary, secondary, and tertiary reflective optics). This is consistent with loading expected due to spillover and pickup due to rms surface errors.

Correlated noise due to atmospheric fluctuations was present in the data, and during some observations dominated the instrument noise at all frequencies of interest. While we anticipate this noise will be reduced during science observations outside of the Bolivian winter, the data were useful for testing principle component analysis based removal of correlated noise; our preliminary results indicate that we can reduce atmospheric noise by more than an order of magnitude with this method as shown in Fig. 7.

5. Current status and plans

The APEX-SZ receiver is currently back in North America being upgraded and characterized for its science deployment, scheduled for late Fall 2006. All detector channels share the same filter stack and thus will be deployed initially with the single-color 150 GHz configuration. Future runs may use a different band-center. The major receiver upgrades are (1) improved bolometer cavity design to improve optical efficiency and cross-talk, (2) installation of six bolometer wedges, constituting 320 TES bolometers, (3) implementation of the full frequency-domain multi-

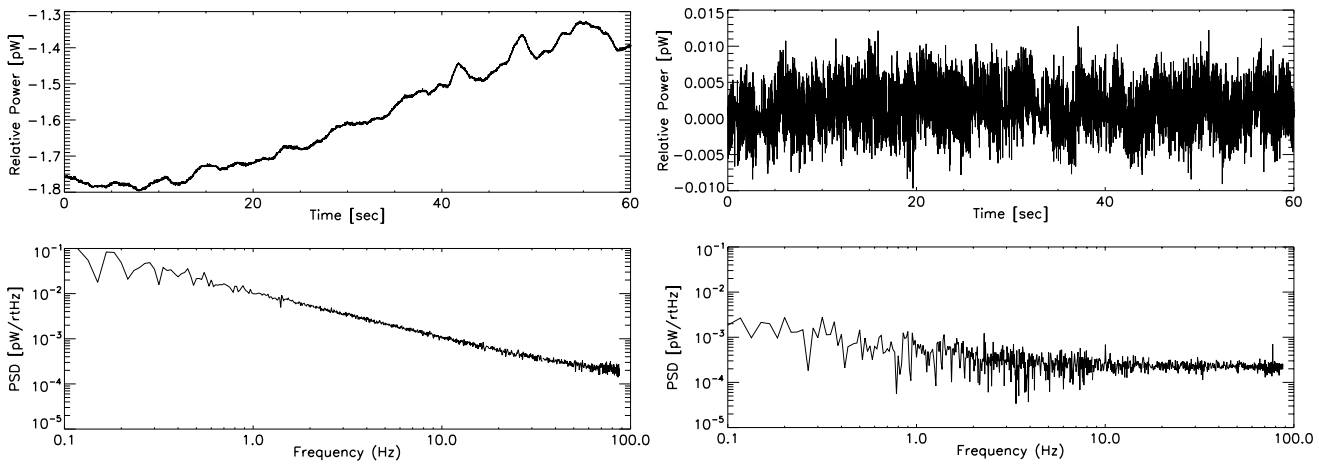

Fig. 7. Timestream and power spectrum density sky-data is shown for one bolometer channel. The raw data plots on the left are dominated by atmospheric fluctuations. The plots on the right show the same data after fitting for the angular wind-speed and subtracting the atmospheric signal with a principle components analysis algorithm.

plexed readout system, with eight bolometer channels per SQUID readout module, (4) improved RF-shielding to further mitigate electromagnetic interference.

Six new bolometer wedges are being fabricated for the science deployment. The bolometers differ from those used in the engineering deployment in two ways. First, the gold spiderweb absorber thickness has been adjusted to give a sheet resistance of 250 Ω/sq. Second, the wedge thickness will be changed to give a backshort distance of 740 μm in silicon. These new values have been optimized with finite-element electromagnetic simulations and are expected to substantially improve the optical efficiency and pixel-to-pixel crosstalk.

Implementation of the eight channel multiplexed readout requires two modifications to the system. The bolometer channels are joined together (implementing the dashed lines in Fig. 4) by redesigning a printed circuit board that is used for mounting the inductors and capacitors for the tuned LCR circuit. This modification is straight-forward. Once the bolometer channels are joined together, inductance from wiring between the LC circuit and SQUID is no longer tuned out by the capacitor. This wiring will be replaced with low-inductance striplines.

The RF-integrity of the detector and SQUID cavity in the receiver is being upgraded by inserting an RF baffling system between this cavity and the optics chamber which is open to the sky through the receiver window.

These improvements are proceeding in parallel and are expected to be implemented and tested in time for a late Fall 2006 science deployment.

6. Conclusion

The APEX-SZ instrument was deployed on the APEX telescope at the Chajnantor site in Chile December 2005–January 2006 for its first light engineering characterization. The instrument was a scaled-down version of the full APEX-SZ concept, having 1/6 of the focal plane instrumented with an AC-biased readout system. Over the course of the ~5 nights of useful observation weather, the bolometer, readout and optics systems were characterized. During this deployment, typically ~43 out of the instrumented 55 Transition Edge Sensor bolometers were recording astronomical signals on the sky. The bolometers were biased with MHz sinusoidal carriers, demonstrating all of the components of the frequency-domain multiplexer system without the final step of joining the bolometers together into a multiplexed comb. The system was cooled without expendable cryogens using a mechanical pulse-tube cooler and three stage He sorption fridge. These achievements are a large step towards future large-scale bolometer array experiments.

Acknowledgements

We acknowledge the exceptional support provided by the APEX site staff led by Lars-Åke Nyman, in particular the extensive engineering efforts of Juan Fluxa, Rodrigo Olivares, Carlos Duran, and Jorge Santana. We also acknowledge the superb efforts of the LBNL engineering division, including John Joseph and Chinh Vu. Frederic Schuller has been instrumental in the development of the Bolometer Data Analysis project (BoA). We thank John Clarke at the University of California, Berkeley for his extensive contributions to the SQUID-based readout. We thank Alex Fletcher and Dan Becker at the University of Colorado at Boulder for current software efforts. This work is supported by National Science Foundation under Grant No. AST-0138348. Work at LBNL is supported by the Director, Office of Science, Office of High Energy and Nuclear Physics, of the US Department of Energy under Contract No. DE-AC02-05CH11231.

References

Güsten, R., Nyman, L.Å., Schilke, P., Menten, K., Cesarsky, C., Booth, R., 2006. The Atacama Pathfinder EXperiment (APEX) – a new

submillimeter facility for southern skies. A & A 454 (August), L13–L16.

Güsten, R., Booth, R.S., Cesarsky, C., Menten, K.M., Agurto, C., Anciaux, M., Azagra, F., Belitsky, V., Belloche, A., Bergman, P., De Breuck, C., Comito, C., Dumke, M., Duran, C., Esch, W., Fluxa, J., Greve, A., Hafok, H., Häupl, W., Helldner, L., Henseler, A., Heyminck, S., Johansson, L.E., Kasemann, C., Klein, B., Korn, A., Kreysa, E., Kurz, R., Lapkin, I., Leurini, S., Lis, D., Lundgren, A., Mac-Auliffe, F., Martinez, M., Melnick, J., Morris, D., Muders, D., Nyman, L.A., Olberg, M., Olivares, R., Pantaleev, M., Patel, N., Pausch, K., Philipp, S.D., Philipps, S., Sridharan, T.K., Polehampton, E., Reveret, V., Risacher, C., Roa, M., Sauer, P., Schilke, P., Santana, J., Schneider, G., Sepulveda, J., Siringo, G., Spyromilio, J., Stenvers, K.-H., van der Tak, F., Torres, D., Vanzi, L., Vassilev, V., Weiss, A., Willmeroth, K., Wunsch, A., Wyrowski, F. 2006. APEX: the Atacama Pathfinder EXperiment. In: Larry M. Stepp (Ed.), Ground-based and Airborne Telescopes. Proceedings of the SPIE, vol. 6267, pp. 626714.

Sunyaev, R.A., Zeldovich, Ya.B., 1970. Small scale fluctuations of relic radiation. Astrophys. Space Sci. 7, 3–19.

Lee, A.T., Cho, S., Gildemeister, J.M., Halverson, N., Holzapfel, W.L., Mehl, J., Myers, M.J., Lanting, T., Richards, P.L., Rittweger, E., Schwan, D., Spieler, H., Tran, H., 2003. Voltage-biased TES bolometers for the far-infrared to millimeter wavelength range. In: Phillips, T.G., Zmuidzinas, J. (Eds.), Millimeter and Submillimeter Detectors for Astronomy. Proceedings of the SPIE, vol. 4855, pp. 129–135.

Spieler, H., 2002. Frequency domain multiplexing for large scale bolometer arrays. In: Wolf, J. Farhoomand, J., McCreight, C.R. (Eds.), Monterey Far-IR, Sub-mm and mm Detector Technology Workshop proceedings, pp. 243–249. NASA/CP-2003-21140 and LBNL-49993, http://www-library.lbl.gov/docs/LBNL/499/93/PDF/LBNL-49993.pdf.

Radford, S.J., Holdaway, M.A., 1998. Atmospheric conditions at a site for submillimeter-wavelength astronomy. In: Phillips, T.G., (Ed.), Proceedings of the SPIE, vol. 3357, pp. 486–494, Advanced Technology MMW, Radio, and Terahertz Telescopes.

Lay, O.P., Halverson, N.W., 2000. The impact of atmospheric fluctuations on degree-scale imaging of the cosmic microwave background. ApJ 543 (November), 787–798.

Miller, A., Beach, J., Bradley, S., Caldwell, R., Chapman, H., Devlin, M.J., Dorwart, W.B., Herbig, T., Jones, D., Monnelly, G., Netterfield, C.B., Nolta, M., Page, L.A., Puchalla, J., Robertson, T., Torbet, E., Tran, H.T., Vinje, W.E., 2002. The QMAP and MAT/TOCO experiments for measuring anisotropy in the cosmic microwave background. ApJS 140 (June), 115–141.

Padin, S., Shepherd, M.C., Cartwright, J.K., Keeney, R.G., Mason, B.S., Pearson, T.J., Readhead, A.C.S., Schaal, W.A., Sievers, J., Udomprasert, P.S., Yamasaki, J.K., Holzapfel, W.L., Carlstrom, J.E., Joy, M., Myers, S.T., Otarola, A., 2002. The cosmic background imager. PASP 114 (January), 83–97.

Kosowsky, A., 2003. The Atacama cosmology telescope. New Astronomy Review 47 (December), 939–943.

Lanting, T.M., Cho, Hsiao-Mei, Clarke, John, Dobbs, Matt A., Lee, Adrian T., Lueker, M., Richards, P.L., Smith, A.D., Spieler, H.G., 2004. Frequency domain multiplexing for bolometer arrays. Nuclear Instruments and Methods in Physics Research A 520, 548–550.

Irwin, K., 1995. An application of electrothermal feedback for high-resolution cryogenic particle-detectors. Applied Physics Letters 66, 1998.

Huber, M.E., Neil, P.A., Benson, R.G., Burns, D.A., Corey, A.F., Flynn, C.S., Kitaygorodskaya, Y., Massihzadeh, O., Martinis, J.M., Hilton, G.C., 2001. DC SQUID series array amplifiers with 120 MHz bandwidth (corrected). IEEE Transactions on Applied Superconductivity 11, 4048–4053.

Ruhl, J.E., Ade, P.A.R., Carlstrom, J.E., Cho, H.M., Crawford, T., Dobbs, M., Greer, C.H., Halverson, N.W., Holzapfel, W.L., Lanting, T.M., Lee, A.T. Leong, J., Leitch, E.M., Lu, W., Lueker, M., Mehl, J., Meyer, S.S., Mohr, J.J., Padin, S., Plagge, T., Pryke, C., Schwan, D., Sharp, M.K., Runyan, M.C., Spieler, H., Staniszewski, Z., Stark, A.A., 2004. The south pole telescope. In: Zmuidzinas, J., Holland, W., Withington, S. (Eds.), Millimeter and Submillimeter Detectors for Astronomy II, Proceedings of the SPIE, vol. 5498, Bellingham, WA, SPIE, pp. 11–29.

Lamarre, J.M., 1986. Photon noise in photometric instruments at far-infrared and submillimeter wavelengths. Applied Optics 25, 870.

Marcus, C., Runyan, et al., 2003. The arcminute cosmology bolometer array receiver. Astrophysics Journal Supplement 149, 265.